SARCOIDOSIS VASCULITIS AND DIFFUSE LUNG DISEASES 2013; 30; 52-59

Differentiation of lymphoma versus sarcoidosis in the setting of mediastinal - hilar lymphadenopathy: assessment with diffusion-weighted MR imaging

S. Gümüştaş[1], N. İnan[1], Gür Akansel[1], İ. Başyiğit[2], E. Çiftçi[1]

[1] Department of Radiology, School of Medicine, University of Kocaeli, Turkey; [2] Department of Chest Diseases, School of Medicine, University of Kocaeli, Turkey

Abstract. *Objectives:* To determine the performance of diffusion-weighted magnetic resonance imaging in differentiating lymphoma from sarcoidosis in mediastinal-hilar lymphadenopathy. *Materials and Methods:* Forty-four mediastinal-hilar lymphadenopathy were examined in 27 patients with T1- and T2-weighted conventional images. Then, two diffusion-weighted images were obtained with b = 0 and 1000 s/mm² values and apparent diffusion coefficients (ADCs) were calculated. The statistical significance of differences between measurements was tested using the Student-t test. *Results:* The ADC value in the lymphoma group was lower than in the sarcoidosis group, and the difference was statistically significant ($p < 0.001$). By using the cut-off value of 1.266 x 10^{-3} mm²/s, ADC had a sensitivity of 100%, specificity of 81%, positive predictive value of 100%, and negative predictive value of 77% for the differentiation of lymphoma and sarcoidosis. With the cut-off value of 1,97 x 10^{-3} mm²/s, ADC had a sensitivity of 50%, specificity of 99.4%, positive predictive value of 68%, and negative predictive value of 91%. *Conclusions:* Diffusion-weighted imaging may be useful besides other modalities in differentiating lymphoma from sarcoidosis in mediastinal-hilar lymphadenopathy. *(Sarcoidosis Vasc Diffuse Lung Dis 2013; 30: 52-59)*

Key words: sarcoidosis, lymphoma, diffusion-weighted imaging, lymph node, magnetic resonance imaging

Introduction

Lymphadenopathy is the most common cause of multiple mediastinal mass (1). Mediastinal-hilar lymphadenopathy has a wide spectrum of differential diagnosis. Lymphoma and sarcoidosis form a great part of the differential diagnosis as the malignant and benign counterparts (2). Distinction is critical because lymphoma is managed with chemotherapy and radiotherapy, while sarcoidosis is generally managed by clinical follow-up or with different therapeutic options such as immunosuppressive therapy. Clinical and laboratory findings are valuable in the differential diagnosis. Typical clinical features such as Löfgren's Syndrome (erythema nodosum skin rash coupled with bilateral hilar adenopathy on chest radiograph and often fever and arthritis) and Heerfordt Syndrome (uveitis, parotidis and fever), presence of lupus pernio, elevation of serum angiotensin converting enzyme levels, presence of subcutaneous nodules suggest the diagnosis of sarcoidosis while night sweats, itching, weight loss mostly suggest the diagnosis of

Received: 6 February 2012
Accepted after Revision: 3 December 2012
Correspondence: Dr. Sevtap Gümüştaş
Kocaeli Uni. Tip Fak Radyoloji AD
41380 Umuttepe Kocaeli, Turkey
Tel. +90 262 3037126
Fax +90 262 303 80 03
E-mail: svtgumustas@hotmail.com

lymphoma (3, 4). Operative methods such as mediastinoscopy and thoracotomy are efficient, but invasive and prone to complications (5). Radiologic differentiation generally depends on computed tomography (CT) findings. There are certain characteristics that have been described for diagnosing sarcoidosis on CT (6-8). Diagnosis can be easy, with symmetrical hilar and mediastinal lymphadenopathy with typical perilymphatically distributed parenchymal nodules. However, in patients with asymmetrical hilar disease and mediastinal lymphadenopathy without hilar disease, the diagnosis can be challenging, mostly mimicking malignancies and especially lymphoma (9). Fluorine-18 fluorodeoxyglucose (FDG) - positron emission tomography (PET)/CT is widely used as a means of malignant-benign differentiation of mediastinal lymph nodes. But this statement can be misleading for sarcoidosis where the lymph nodes can be highly avid (8, 10). Besides, both CT and FDG-PET/CT are techniques that expose the patient to ionizing radiation. Magnetic resonance imaging (MRI) is superior to those methods because it avoids radiation exposure, is non-invasive and can provide excellent soft tissue contrast details. Diffusion-weighted magnetic resonance imaging (DWI) views the microscopic movement and diffusion of water molecules in tissues, which is highly influenced by the cellular water content, intracellular organelles and macromolecules. Thus, DWI provides valuable clues for a functional assessment of tissue microstructure in relation to the anatomy (11). DWI was used in malignant-benign differentiation of mediastinal masses and lympadenopathy in recent reports (12-14). DWI also gives valuable clues regarding malignant involvement of mediastinal lymph nodes in lung cancer (15-19). However, DWI in the differentiation of subgroups lymphoma versus sarcoidosis was never evaluated specifically.

The purpose of this study was to investigate the differentiation of these two diseases in patients with mediastinal- hilar lymphadenopathy by using DWI.

Materials and Methods

Patients

The study was approved by our institutional review board and protocol review committee. Because the tests used were part of the routine clinical workup of these patients, informed consent was not required by the review board. We obtained blanket consent from all patients for the use of their findings for research and educational purposes, with patient privacy secured.

From February 2010 to April 2011, 47 patients with mediastinal-hilar lymphadenopathy were included in our study. Of the 47 patients that were referred to MRI scanning, just 7 patients already had clinically or histopathologically proven diagnosis of sarcoidosis. These 7 patients were followed-up every 3 to 6 months and routine investigations included physical examination, pulmonary function tests. CT scans were performed in order to evaluate parenchymal infiltration and signs of fibrosis if patients have worsening symptoms, abnormal physical examination findings and/or progressive decline in lung functions. They do not have medical therapy currently. These 7 patients did not go any further investigation for diagnosis because they already had. They were included in the study in the sarcoidosis group and underwent MRI scanning prospectively. Remaining 40 patients without a certain diagnosis but were referred to chest CT on clinical suspect of sarcoidosis or lymphoma, were consecutively included in this prospective study according to our exclusion criteria. Our exclusion criteria were as follows; (a) lesions containing large amounts (more than 50 % of total size) of necrosis or calcification; (b**)** lesions size <15 mm in short-axis diameter in view of the limited planar resolution of DWI; (c) patients with known malignancy (d) patients with acute infectious symptoms who were referred to CT scanning for chest infection (e) patients receiving steroids, chemotherapy or radiotheraphy; and (f) contraindications for MRI present. The patient should be able to tolerate the examination and hold breath approximately 26 seconds in the MRI unit.

Of the 47 patients, 16 were excluded because they could not stay still in the MRI unit because of serious respiratory artefacts or claustrophobia. Four patients were excluded because they had final diagnosis of extrathoracic malignant metastasis. Remaining 27 patients (8 males, 19 females) with mediastinal-hilar lymphadenopathy detected on chest CT and had a final diagnosis of sarcoidosis or lymphoma (12 sarcoidosis, 15 lymphoma) were included in this study.

Magnetic Resonance Imaging

All patients were examined using a 3 Tesla (3T) MRI unit (Philips Achieva Intera Release, Eindhoven, The Netherlands), with a four-element phased-array body coil. All patients initially underwent a routine MRI session for the thorax that included: axial T1-weighted (W) breath-hold turbo field echo (TFE) without fat suppression (TR/TE/FA/NEX:10/2.3/15/1) and axial T2-W single-shot turbo spin echo (SS-TSE) (TR/TE/NEX/TSE factor: 1536/80/1/73). Subsequently, two series of axial single-shot spin-echo echo-planar (SS-SE-EPI) DWIs were acquired using the b values 0 and 1000 s/mm² (EPI factor, 57; TR/TE/NEX: 1720/68/2; we used sensitizing gradients in *x*, *y*, and *z* directions in order to obtain isotropic diffusion weighting). Apparent diffusion coefficient (ADC) maps were reconstructed from the b 0 and b 1000 s/mm² images. MRI, including DWI, consisted of a multisection acquisition with a slice thickness of 6 mm, an intersection gap of 1 mm, and an acquisition matrix of 140×108. The field of view varied between 455 and 500 mm. All sequences were acquired using a partially parallel imaging acquisition and SENSE (sensitivity encoding) reconstruction with a reduction factor (*R*) of 2. Each of the b values was obtained during a single breath-hold, and the examination time was 26 seconds for each b value acquisition.

Quantitative analysis

Quantitative measurements were made using a dedicated workstation (Dell Workstation Precision 650, with the View Forum software platform provided by Philips Healthcare). All images were assessed by two radiologists (S.G., N.I.) who were blinded to the clinical history and results of the prior imaging studies. Each lesion was first evaluated on conventional images for location, size and the presence of cystic-necrotic parts. We did not do any analyses on conventional images; they were used only to identify the lesion. Afterwards, ADCs were calculated from the ADC maps, which were reconstructed from b = 0 and b = 1000 s/mm² values. A ROI was drawn centrally, and the size of ROI was kept as large as possible on the ADC map avoiding the macroscopic necrosis and major blood vessels in the light of the conventional images. The average of three measurements was recorded as the final result.

Statistical analysis

The ADC values were compared between the groups. The Kolmogorov-Smirnov test showed that the data were normally distributed, so the differences in ADCs were analysed using the Student-t test. A *p* value of less than 0.05 was considered statistically significant. To evaluate the diagnostic performance of the mean ADC measurements in differentiating malignant from benign lesions and to describe the sensitivity and specificity, receiver operating characteristic (ROC) analysis was performed. An optimum cut-off point was hence determined as the value that best discriminates between the two groups in terms of maximum sensitivity and minimum number of false-positive results. All statistical analyses were performed using statistical software (Statistical Package for the Social Sciences [SPSS] version 15).

Results

Patients

The mean age of the entire group was 45 ± 24 years (range: 19-61 years). The mean age of patients with sarcoidosis was 39 ± 19 years (range: 26 - 56 years) and of patients with lymphoma was 44 ± 21 years (range: 19 - 61 years). The difference in age between groups was not statistically significant (p = 0.5).

The mean diameter of lymphadenopathy for the entire group was 27 ± 18 mm. The mean diameter of sarcoidosis was 24 ± 9 mm (range: 15 - 35 mm) and of lymphoma was 33 ± 19 mm (range: 15 - 60 mm). The difference in diameter between the groups was not statistically significant (p = 0.1).

Diagnosis

All 27 patients had lymphadenopathy, but only lesions appropriate to the criteria were measured (number of total lymph nodes measured = 44). Of the 44 lymphadenopathies, 23 were lymphoma (14 were Hodgkin and 9 were non-Hodgkin lymphomas) and 21 were sarcoidosis.

Of the 23 nodes in the lymphoma group; 2 nodes were measured in 5 patients (10 lymphadenopathy) and 4 nodes were measured in 1 patient (4 lymphadenopathy). The remaining 9 patients each had one node measured (9 lymphadenopathy). Of the 21 nodes in the sarcoidosis group; 2 nodes were measured in 4 patients (8 lymphadenopathy), 3 and 4 nodes were measured in 2 patients (7 lymphadenopathy). A single node was evaluated in the remaining 6 patients (6 lymphadenopathy).

Lymph nodes localized and defined according to UICC were as follows: in the lymphoma group; 4 hilar, 6 lower paratracheal, 6 subcarinal, 7 para-aortic, and in the sarcoidosis group; 5 hilar, 7 lower paratracheal, 5 subcarinal, 4 para-aortic. Hilar nodes were more measurable with respect to diameter in the sarcoidosis group and mediastinal nodes were more measurable in the lymphoma group, but the difference in size was not statistically significant (p = 0.1).

In the lymphoma group (15 patients), pathologic evidence was available in all patients by either percutaneous, transbronchial or excisional biopsy.

In the sarcoidosis group (12 patients), pathologic evidence was obtained in 7 patients as non-caseating granulomas. Three sarcoidosis patients were diagnosed based on CT images and clinical parameters. Those 3 patients were diagnosed as Löfgren's syndrome with erythema nodosum, bilateral hilar adenopathy and fever. Histopathological confirmation could not be performed because of patients' non-compliance and sarcoidosis was diagnosed based on their typical presentation and radiological findings. Remaining two sarcoidosis patients had typical bronchoalveolar lavage findings during bronchoscopy that helped to confirm the diagnosis**.** Lymphocyte predominant bronchoalveolar lavage fluid with increased CD4/CD8 ratio (>3.5) was suggested as typical bronchoalveolar lavage finding for sarcoidosis. None of the patients were under treatment when MRI was performed. In all cases, MRI was performed prior to invasive mediastinal procedures.

Findings on DWI

We could obtain an ADC value for all lymph nodes. The results of the quantitative analysis of ADC values with pathologic diagnosis are reviewed in Table 1 and 2.

ADC analysis

The mean ADC for lymphoma was 1.130 ± 0.581 $x10^{-3}$ mm^2/s and for sarcoidosis was 2.065 ± 0.518 $x10^{-3}$ mm^2/s (Fig. 2). The difference in ADC values between lymphoma and sarcoidosis was statistically significant ($p < 0.001$) (Fig. 3). The difference in ADC values between Hodgkin and non-Hodgkin lymphomas was not statistically significant (p = 0.3).

ROC curve analysis

The area under the ROC curve was 0.83 ± 0.70 ($p < 0.001$) for ADC value (Fig. 4). With a cut-off value of 1.266 x 10^{-3} mm^2/s, ADC had a sensitivity of 100%, and specificity of 81%, positive predictive value of 100%, and negative predictive value of 77% for the differentiation of lymphoma and sarcoidosis. When the cut-off value is higher as 1,97 x 10^{-3} mm^2/s, ADC had a sensitivity of 50%, specificity of 99.4%, positive predictive value of 68%, and negative predictive value of 91%. We achieved higher specificity but markedly lower sensitivity.

Among the sarcoidosis group, all ADC values were above the cut-off value and there were no false-positive results. Six lesions among 23 malignant lymphadenopathy (4 Hodgkin lymphoma, 2 non-Hodgkin lymphoma) revealed ADC value >1.266 x 10^{-3} mm^2/s, which could be confused as benign.

Table 1. Diagnosis and quantitative analysis of DW imaging of lymph nodes (median ADC values obtained from b = 0 and 1000 s/mm^2)

Diagnosis	Lymphoma (n = 23)	Sarcoidosis (n = 21)	P
ADC ($x10^{-3}$) mm^2/s	1.130 ± 0.581	2.065 ± 0.518	***0.001***

Table 2. Diagnosis and quantitative analysis of DW imaging of lymph nodes (median ADC values obtained from b = 0 and 1000 s/mm^2)

Diagnosis	Hodgkin lymphoma (n = 14)	Non-hodgkin lymphoma (n = 9)	P
ADC ($x10^{-3}$) mm^2/s	1.198 ± 0.583	1.115 ± 0.581	0.3

Note: Data are mean ± SD

Discussion

Differential diagnosis of mediastinal-hilar lymphadenopathy is an issue of debate for radiologists, especially in cases suspicious for lymphoma versus sarcoidosis. CT has been widely used but is not sufficient for malignant-benign differentiation. Although FDG–PET/CT is helpful in the differential diagnosis, lymph nodes in sarcoidosis can sometimes show marked FDG uptake, and this can be misdiagnosed as malignant (8, 10). In a recent study, F-18-methyltyrosine (FMT)-PET was used in combination with FDG-PET, and authors found that this can be an effective method to distinguish sarcoidosis from malignancy in patients with hilar lymphadenopathy (20). In this report, FDG-PET showed increased uptake in all sarcoidosis patients where FMT-PET showed normal uptake in all of them.

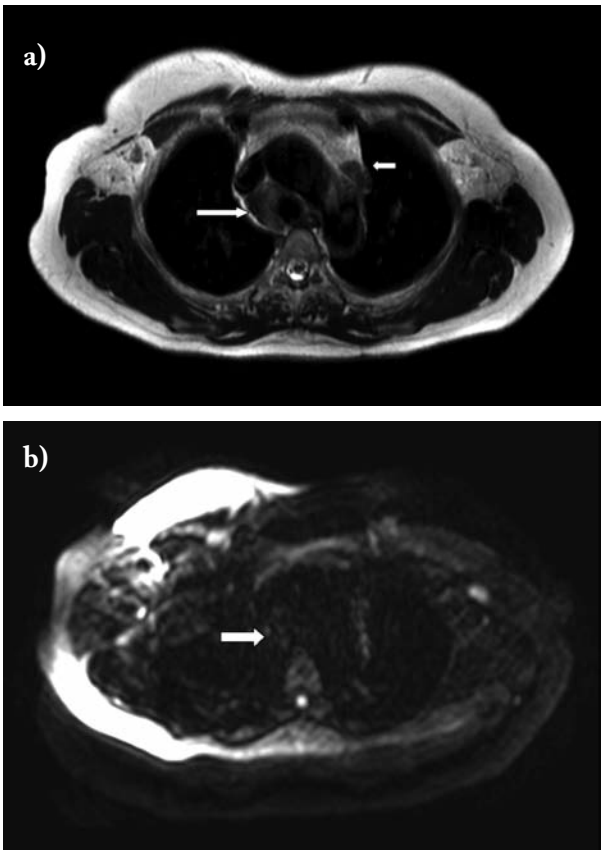

Fig. 1. Sarcoidosis, 54-year-old woman with multiple hilar and mediastinal lymphadenopathies. **a)** Transversal T2-W single-shot turbo spin echo image shows lymphadenopathy in station 4R (right lower paratracheal) (arrow) and lymph nodes in station 6 (para-aortic) (short arrow) **b)** Single-shot spin-echo echo-planar DW image shows lymphadenopathy in station 4R is nearly invisible with low intensity (arrow) **c** ADC map, notice the lymphadenopathy shows significant high intensity (1.83 x10^{-3} mm²/s) (curved arrow)

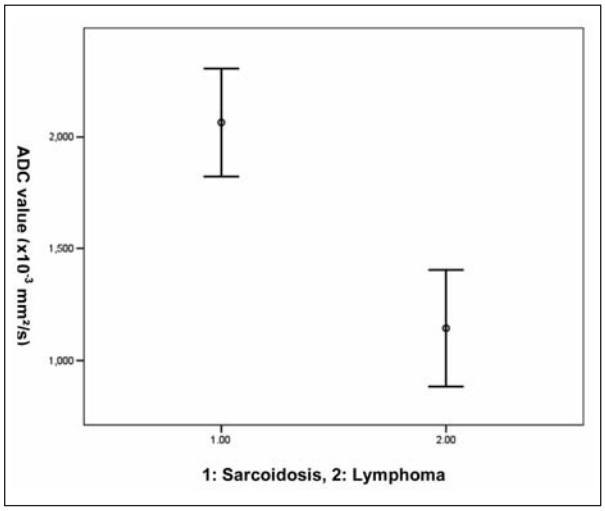

Fig. 2. Comparison of ADC values (x10^{-3} mm²/s) from b =0 and 1000 s/mm² between lymphoma and sarcoidosis. The mean ADC value of lymphoma was significantly lower than those of sarcoidosis

MRI has been used to differentiate metastatic versus non-metastatic nodes in the mediastinum. Short inversion time inversion-recovery (STIR) turbo spin-echo (TSE) MRI was found valuable in differentiating lymph nodes with metastasis from those without (21, 22). Malignant and benign differentiation of mediastinal lymphadenopathy with DWI was investigated recently in some studies (12, 15-19). In two different reports Abdelrazek et al. (12) and Ko ucu et al. (19) investigated mediastinal lymphadenopathy in variable malignant and benign diseases, and found that DWI can be used for malignant nodal differentiation. In the reports of Usuda et al. (15) and Nomori et al. (16), nodal staging of lung cancer was compared between DWI and FDG-PET/CT and the authors found that DWI can be used instead of FDG-PET/CT as a means of metastatic and non-metastatic lymph node differentiation. Nakayama et al. (17) quantitatively measured DWI in lymph nodes in non-small cell lung carcinoma, and found a significant difference between metastatic and non-metastatic nodes. Hasegawa et al. (18) stated that low DWI SI in lymph nodes cor-

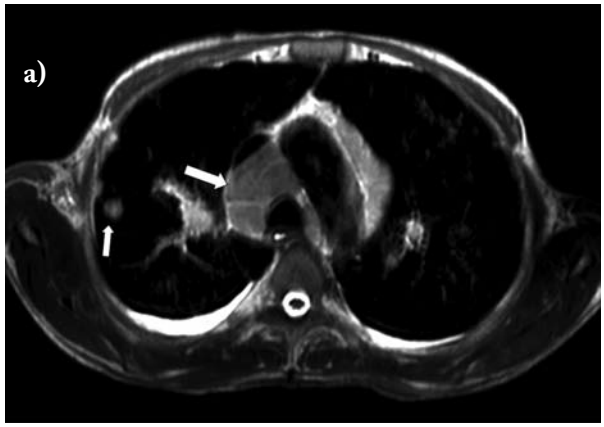

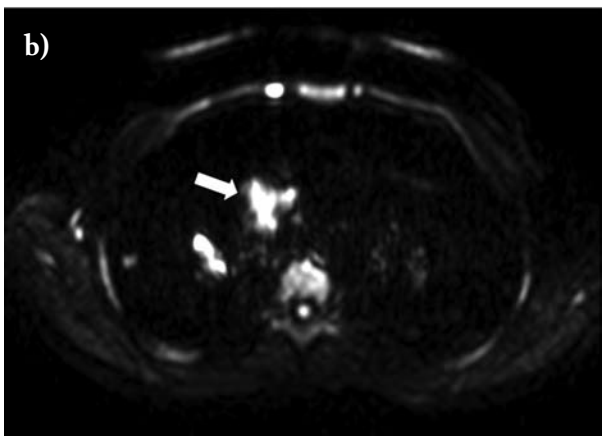

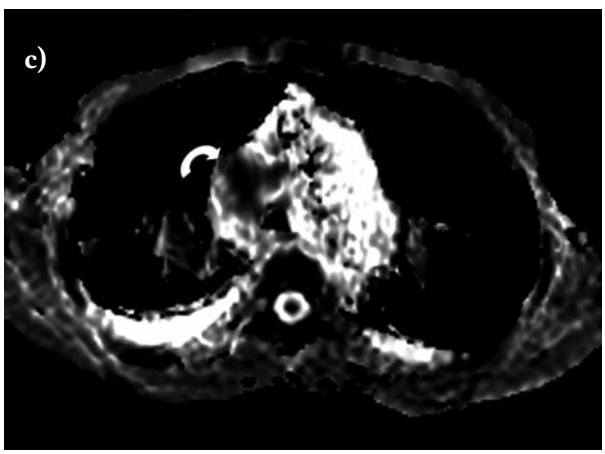

Fig. 3. Hodgkin disease, a 61-year-old man with multiple hilar and mediastinal lymphadenopathies. **a)** The lymphadenopathy in station 4R (right lower paratracheal) is slightly hyperintense on T2-W single-shot turbo spin echo image (arrow). There are also some metastatic nodules in the upper lobes (short arrow) and bilateral pleural effusions. **b)** Single-shot spin-echo echo-planar DW image shows the lymphadenopathy has significantly high signal intensity (arrow). **c)** The lymphadenopathy shows significant low intensity on ADC map with low ADC value (1.09 x10^{-3} mm^2/s) (curved arrow)

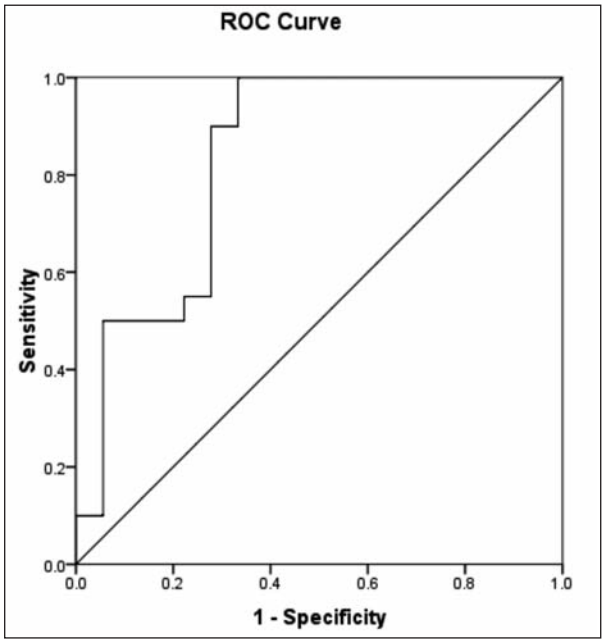

Fig. 4. ROC curve for ADC measurements for the determination of sarcoidosis and lymphoma. Area under the ROC curve was 0.83 ± 0.70

responding to conventional T2-W images is valuable for diagnosing metastatic involvement in non-small cell lung cancer. In the English literature, there is no specific study that evaluated only subgroups of lymphoma and sarcoidosis.

In our study, we evaluated mediastinal-hilar lymphadenopathy in subgroups of lymphoma and sarcoidosis. All the studies mentioned above were performed with 1.5 Tesla MRI systems (12, 15-19). To our knowledge, the role of DWI in the differentiation of mediastinal lymph nodes has not been reported at a 3T system. Theoretically, the major advantage of 3T systems should be the higher signal-to-noise ratio (SNR) which translates into higher temporal and spatial resolution (23). The authors experience is that increased SNR at 3T improves the quality of DWI. We believe that our results are encouraging for a potential role for high b value diffusion weighted imaging in the differentiation of mediastinal nodes with the advantages of higher SNR.

In our study, we analysed ADC values and found significant difference between lymphoma and sarcoidosis ($p < 0.001$). Most lymphomas are hypercellular, with enlarged nuclei and hyperchromatism, which result in a contracted extracellular space and

decreased ADC (24). However, the ADC may be misleadingly elevated depending on differences between lymphoma types in cellularity, intracellular architecture, the presence and amount of necrosis, and perfusion. This may explain why 6 cases of lymphoma displayed ADC results above the cut-off value of 1.266 x 10^{-3} mm^2/s, while there were no false positives. Of the six lymph nodes with false negative results, two were non-Hodgkin lymphoma nodes from the same patient, with no macroscopic necrosis on conventional MRI, but with microscopically necrobiotic tissue proven histopathologically. Two other false-negative nodes were measured from one patient with Hodgkin lymphoma with macroscopically necrotic and non-necrotic nodes observed adjacent to the ones measured on MRI. This was the only patient with lymph nodes containing more than 50% necrosis in some of the nodes although these nodes were not chosen for measurement. Despite the fact that only non-necrotic nodes were measured on DWI, we suspect that these apparently non-necrotic nodes may include areas of microscopic necrosis at least in some of the patients, which may ultimately limit the use of this technique in patients with macroscopically necrotic nodes elsewhere. Further studies are required to document if this is the case. Remaining two nodes were from two separate patients with Hodgkin lymphoma. None had evidence for macroscopic necrosis elsewhere. We have no plausible explanation for the elevated ADC values observed in these patients. These initial results of our study need to be confirmed in larger patient series by MRI.

In a few studies no significant difference was observed between ADCs of indolent lymphoma and aggressive lymphomas or non-Hodgkin lymphoma and Hodgkin lymphoma (25, 12). We also did not find any significant difference between non-Hodgkin and Hodgkin types.

The main limitation of our study is susceptibility artefacts that can result in image non-uniformities including distortion. These artefacts increase with the main magnetic field strength and are supposed to be more problematic on 3T systems. DWI at high field strength is typically obtained using EPI sequences (single-shot and multishot). The single-shot technique is inherently prone to susceptibility artefacts, which are exacerbated by the presence of metal and air. To reduce these artefacts, modern 3T systems routinely apply parallel imaging techniques, which decrease echospacing and echo-train length as we also used. Multishot EPI sequences are inherently less sensitive to susceptibility and are therefore increasingly being used for 3T DWI. We experienced that artefacts are more prominent on the images of thoracic inlet and basal lung segments, but less bothersome on the images of middle zone mediastinum, where we estimated our results, especially with patients having massive lymphadenopathy. Although it has been mentioned in some studies (19, 24) that low b values reduce susceptibility artefacts, it must be kept in mind that low b values also reduce the diffusion effect. In our study, we used high b values in order to obtain reliable diffusion results, and we could keep the quality of our data at reasonable levels.

In sarcoidosis group histopathological proof was available in only 7 patients. Although it is certainly desirable to obtain histopathological evidence, it is also considered standard practise to make the diagnosis of sarcoidosis using combinations of positive clinical, radiological and laboratory findings (4).

In some patients we analysed multiple lymph nodes (4 nodes were measured in 2 patients and 3 nodes were measured in 1 patient). This probably can be a limitation because we have a small cohort of patients. Another limitation is the size of the lymph nodes evaluated. Small-size nodes were excluded from the study because quantitative assessments require a large area in order to obtain accurate results.

In conclusion, we suggest that ADC measurements on DWI may be helpful besides CT images in differentiating lymphoma from sarcoidosis in mediastinal-hilar lymphadenopathy noninvasively.

References

1. Fraser RS, Pare JAP, Fraser RG, Pare PD. Diseases of the chest. Philadelphia: WB Saunders, 1994.
2. Webb WR, Higgins CB. Thoracic imaging: pulmonary and cardiovascular radiology. Philadelphia: Lippincott Williams and Wilkins, 2010. Second edition.
3. Judson MA. Sarcoidosis: clinical presentation, diagnosis, and approach to treatment. Am J Med Sci 2008; 335: 26-33.
4. Baughman RP, Culver DA, Judson MA. A concise review of pulmonary sarcoidosis. Am J Respir Crit Care Med 2011; 183: 573-81.
5. Nguyen BC, Stanford W, Thompson BH, Rossi NP, Kernstine KH, Kern JA, et al. Multicentre clinical trial of ultra- small super paramagnetic iron oxide in the evaluation of mediastinal lymph nodes in patients with primary lung carcinoma. J Magn Reson Imaging 1999; 10: 468-73.

6. Nishino M, Lee KS, Itoh H, Hatabu H. The spectrum of pulmonary sarcoidosis: variations of high-resolution CT findings and clues for specific diagnosis. Eur J Radiol 2010; 73: 66-73.
7. Balan A, Hoey ET, Sheerin F, Lakkaraju A, Chowdhury FU. Multitechnique imaging of sarcoidosis. Clin Radiol 2010; 65: 750-60.
8. Prabhakar HB, Rabinowitz CB, Gibbons FK, O'Donnell WJ, Shephard JAO, Aquino SL. Imaging features of sarcoidosis on MDCT, FDG PET, and PET/CT. Am J Roentgenol 2008; 190: 1-6.
9. Suwatanapongched T, Gierada DS. CT of thoracic lymph nodes. Part II: diseases and pitfalls. Br J Radiol 2006; 79: 999-1006.
10. Krüger S, Buck AK, Mottaghy FM, et al. Use of integrated FDG-PET/CT in sarcoidosis. Clin Imaging 2008; 32: 269-73.
11. Henzlera T, Schmid-Bindertb G, Schoenberga SO, Finka C. Diffusion and perfusion MRI of the lung and mediastinum. Eur J Radiol 2010; 76 (3): 329-36.
12. Abdel Razek A, Elkammary S, Elmorsy A, Elshafey M, Elhadedy T. Characterization of mediastinal lymphadenopathy with diffusion-weighted imaging. Magn Res Imag 2011; 29: 167-72.
13. Gumustas S, Inan N, Sarisoy HT, et al. Malignant versus benign mediastinal lesions: quantitative assessment with diffusion weighted MR imaging. Eur Radiol 2011; 21: 2255-60.
14. Abdel Razek A, Elmorsy A, Elshafey M, Elhadedy T, Hamza O. Assessment of mediastinal tumors with diffusion-weighted single-shot echo-planar MRI. J Magn Reson Imaging 2009; 30: 535-40.
15. Usuda K, Zhao XT, Sagawa M, et al. Diffusion-weighted imaging is superior to positron emission tomography in the detection and nodal assessment of lung cancers. Ann Thorac Surg 2011; 91: 1689-95.
16. Nomori H, Mori T, Ikeda K, et al. Diffusion-weighted magnetic resonance imaging can be used in place of positron emission tomography for N staging of non–small cell lung cancer with fewer false-positive results. J Thorac Cardiovasc Surg 2008; 135: 816-22.
17. Nakayama J, Miyasaka K, Omatsu T, et al. Metastases in mediastinal and hilar lymph nodes in patients with non-small cell lung cancer: quantitative assessment with diffusion weighted magnetic resonance imaging and apparent diffusion coefficient. J Comput Assist Tomogr 2010; 34: 1-8.
18. Hasegawa I, Boiselle PM, Kuwabara K, Sawafuji M, Sugiura H. Mediastinal lymph nodes in patients with non-small cell lung cancer: preliminary experience with diffusion-weighted MR imaging. J Thorac Imaging 2008; 23: 157-61.
19. Kosucu P, Tekinbas C, Erol M, et al. Mediastinal lymph nodes: assessment with diffusion-weighted MR imaging. J Magn Reson Imaging 2009; 30: 292-97.
20. Kaira K, Oriuchi N, Otan Y, Yanagitan N, Sunaga N, Hisada T. Diagnostic usefulness of fluorine–18- methyltyrosine positron emission tomography in combination with 18F-fluorodeoxyglucose in sarcoidosis patients. Chest 2007; 131: 1019-27.
21. Ohno Y, Hatabu H, Takenaka D, et al. Metastases in mediastinal and hilar lymph nodes in patients with non–small cell lung cancer: quantitative and qualitative assessment with STIR turbo spin-echo MR imaging. Radiology 2004; 231: 872-79.
22. Takenaka D, Ohno Y, Hatabu H, et al. Differentiation of metastatic versus non-metastatic mediastinal lymph nodes in patients with non-small cell lung cancer using respiratory triggered short inversion time inversion recovery (STIR) turbo spin echo MR imaging. Eur J Radiol 2002; 44: 216-24.
23. Song I, Kim CK, Park BK, Park W. Assessment of response to radiotherapy for prostate cancer: value of diffusion-weighted MRI at 3 T. Am J Roentgenol 2010; 194: 477-82.
24. Matoba M, Tonami H, Kondou T, Yokota H, Higashi K, Toga H, et al. Lung carcinoma: diffusion weighted MR imaging - Preliminary evaluation with apparent diffusion coefficient. Radiology 2007; 243: 570-7.
25. Kwee TC, Ludwig I, Uiterwaal CS, et al. ADC measurements in the evaluation of lymph nodes in patients with non-Hodgkin lymphoma: feasibility study. Magn Reson Mater Phy 2011; 24: 1-8.